Calculation of radial matrix elements and anticrossings for highly excited Stark states using the *B*-spline approach

Hongwei Song and Yong Li*
Department of Physics, Huazhong Normal University, Wuhan 430079, China
(Received 27 August 2008; revised manuscript received 21 October 2008; published 9 December 2008)

The calculation of the radial matrix elements of alkali metal Rydberg states is of interest with principal quantum number n up to 70. Until now calculations of the radial matrix elements have mainly concerned the states with $n<30$. We use *B*-spline expansion technique and model potentials to calculate the radial matrix elements by numerical integration with 16 decimal digits precision. We are able to obtain the radial matrix elements of alkali metal Rydberg states with n up to 145, with five significant digits. As a test example, we also compute the positions and widths of the anticrossings for highly excited Stark states of Na with principal quantum number n up to 70.

DOI: 10.1103/PhysRevA.78.062504 PACS number(s): 31.15.ag

I. INTRODUCTION

The calculation of the radial matrix elements of alkali metal Rydberg states is of interest with principal quantum number n up to 70. In the astrophysical environment, high Rydberg atoms are formed with a wide range of values of the principal quantum number n by radiative recombination process. As a result, theoretical calculations involving transition matrix elements, radiative lifetimes, and oscillator strengths have become important to support experimental results concerning high n states of Rydberg atoms [1]. The multiphoton ionization of alkali metal atoms in strong microwave fields is taken as multistep or rate-limiting step processes; and the ionization threshold is determined by the first transition step [2]. Each step is taken as a multiphoton transition process [3]. To calculate the multiphoton transition, the radial matrix elements of an alkali metal Rydberg state are needed with principal quantum number n up to 70 [4]. Therefore, it is desirable to have a theoretical method to calculate the radial matrix elements of alkali metal Rydberg states with principal quantum number n up to 70 or more.

Until now calculations about the radial matrix elements of alkali metal Rydberg states have mainly concerned the states with principal quantum number $n<30$ [5–7]. The reason may be due to the fact that one of the commonly used methods to calculate the radial matrix elements is the Coulomb approximation. The Coulomb approximation (CA) wave functions or analytical CA method cannot be directly applied to cases with high principal quantum numbers ($n>30$) [8]. To our knowledge, only Li *et al.* [9] have reported a theoretical calculation of the radial matrix elements of Rydberg states of Rb with principal quantum number $n\leqslant 52$, where the wave functions from a kind of atomic potential model are used and the radial matrix elements are computed by direct numerical integration with 32 decimal digits precision.

Recently, *B*-spline has been widely applied to the calculation of atomic and molecular physics [10]. As the first application of *B*-spline basis to atoms in external field, Xi *et al.* [11] calculated the accurate energies of ground and low excited states of a hydrogenic atom in a magnetic field of arbitrary strength. Liu *et al.* [12] computed the spectrum and lifetime of the hydrogen circular states. Rao *et al.* [13] calculated accurate complex energies of low-lying resonances for a wide range of electric-field strength with a *B*-spline basis. Jin *et al.* [14,15] used *B*-spline to study microwave multiphoton transition and anticrossings of potassium Rydberg states. Numerous applications of the *B*-spline basis algorithm show the power of *B*-spline functions in theoretical calculations.

The purpose of the present paper is to explore the approach to calculate the radial matrix elements of alkali metal Rydberg states with higher principal quantum number n. We use *B*-spline expansion technique and a parametric model potential to calculate the radial matrix elements by numerical integration with 16 decimal digits precision. We are able to obtain the radial matrix elements of alkali metal Rydberg states with n up to 145, with five significant digits which is accurate enough for all applications. As a test example, we also compute the positions and widths of the anticrossings for highly excited Stark states of Na with principal quantum number n up to 70 and compare the results with other ones whenever available.

II. METHOD

The Hamiltonian for an alkali metal atom is as follows (in atomic units):

$$H_0 = -\tfrac{1}{2}\nabla^2 + V(r), \tag{1}$$

where $V(r)$ is the one-electron parametric model potential which includes the short-range correlation effect given by Marinescu *et al.* [16] and takes the form

$$V_l(r) = -\frac{Z_l(r)}{r} - \frac{\alpha_c}{2r^4}(1 - e^{-(r/r_c)^6}), \tag{2}$$

where α_c is the static dipole polarizability of the positive-ion core, and the radial charge $Z_l(r)$ is given by

*Corresponding author; yongli@phy.ccnu.edu.cn

TABLE I. Optimized parameters for the l-dependent model potential of Na (reproduced from Table 1 of Ref. [16]).

	a_1	a_2	a_3	a_4	r_c	α_c
$l=0$	4.82223117	2.45449865	−1.12255048	−1.42631393	0.45489422	0.9448
$l=1$	5.08382502	2.18226881	−1.19534623	−1.03142861	0.45798739	
$l=2$	3.53324124	2.48697936	−0.75688448	−1.27852357	0.71875312	
$l\geqslant 3$	1.11056646	1.05458759	1.73203428	−0.09265696	28.6735059	

$$Z_l(r) = 1 + (z-1)e^{-a_1 r} - r(a_3 + a_4 r)e^{-a_2 r}, \tag{3}$$

where z is the nuclear charge of the neutral atom and r_c is the cutoff radius introduced to truncate the unphysical short-range contribution of the polarization potential near the origin. The optimized parameters in (2) and (3) are listed in Table I (reproduced from Table 1 of Ref. [16]). This model potential can well describe the motion of the valence electron for the alkali metal atoms.

To obtain the radial matrix elements, we need the eigenfunctions of the Hamiltonian (1). We tackle this eigenvalue problem with the conventional diagonalization method, in which the bases are chosen from B-splines.

Given a knot sequence on the r axis $\{r_1 \leqslant r_2 \leqslant r_3 \leqslant \cdots \leqslant r_N \leqslant \cdots \leqslant r_{N+k}\}$, B-spline function of order k is defined as [17]

$$B_{i,1}(r) = \begin{cases} 1, & r_i \leqslant r < r_{i+1}, \\ 0, & \text{otherwise}, \end{cases}$$

$$B_{i,k}(r) = \frac{r - r_i}{r_{i+k-1} - r_i} B_{i,k-1}(r) + \frac{r_{i+k} - r}{r_{i+k} - r_{i+1}} B_{i+1,k-1}(r) \quad (k > 1). \tag{4}$$

It is immediately seen that $B_{i,k}$ is piecewise polynomial of order $k-1$ localized within (r_1, r_{N+k}), while $B_{i,k}$ is nonvanishing only within (r_i, r_{i+k}). The behavior of the B-spline functions can be readily adjusted with the knot sequence, viz., the choice of knot point r_i, order k, and number of B-splines N, which offers a means to optimize the B-splines as a basis set to expand the wave functions.

The radial wave function $R_{nl}(r)$ of Hamiltonian (1) can be constructed with the B-splines as a basis set,

$$R_{nl}(r) = \sum_{i=1}^{N} C_i B_{i,k}(r). \tag{5}$$

Substituting $R_{nl}(r)$ and $V_l(r)$ into the radial Schrödinger equation of Hamiltonian (1), we obtain

$$\bar{H}\bar{C} = E\bar{S}\bar{C}, \tag{6}$$

where $\bar{H}$ is the Hamiltonian matrix and $\bar{S}$ is the overlap matrix of B-splines. E and $\bar{C}$ are eigenvalues and eigenvectors, respectively. Solving this generalized eigenvalue equation, we obtain the radial wave functions that have correct number of nodes.

The Hamiltonian for an alkali metal atom subject to a static field F along the z axis is as follows (in atomic units):

$$H = -\tfrac{1}{2}\nabla^2 + V(r) + Fz. \tag{7}$$

Using the above zero-field wave functions as a basis, the matrix elements of the Hamiltonian (7) have the following form:

$$H_{nlm,n'l'm} = \delta_{nlm,n'l'm} E_{nlm} + F_s \langle nl|r|n'l'\rangle \langle lm|\cos\theta|l'm\rangle, \tag{8}$$

where $\delta_{nlm,n'l'm}$ is a product of Kronecker δ function. Because the off-diagonal matrix element of r decreases rapidly as the energy difference between two corresponding states increases, the bases are chosen only in the vicinity of the studied states. By diagonalizing the matrix of H, the positions and widths of the anticrossings can be obtained.

III. RESULTS AND DISCUSSIONS

Once the eigenfunctions of the Hamiltonian (1) are obtained, we can calculate the radial matrix elements, $\langle nl|r|n'l'\rangle$, by the direct numerical integration with 16 decimal digits precision. To test the precision of the method, we calculate some radial matrix elements for hydrogen. The results are listed in Table II. For comparison with previous calculation, the numerical results from Li *et al.* [9] are also presented in Table II. As $n-l$ increases, due to the fact that the number of nodes and grid points becomes large, numerical integration errors also increase. From Table II we can see that even if $n-l$ is as high as 145, the precision of our numerical integration is at least up to five significant figures. In contrast, the precision of Li *et al.* is only up to five significant figures when $n-l$ reaches to 64, moreover, their results were calculated with 32 decimal digits precision. This means if we calculate the radial matrix elements with 32 decimal digits precision, ones with n more than 145 can be obtained with five significant digits. But the present calculated results are enough for all applications.

As a test example, we compute the positions and widths of the initial anticrossings for highly excited Stark states of Na with principal quantum number n up to 70. The potential used here is the one given by Marinescu *et al.* [16]. According to the analysis of the effects of errors in the matrix elements [19], using our radial matrix elements, the errors due to the precision of numerical integration can be neglected when we calculate the positions and widths of the initial anticrossings of Na Stark states with n up to 145.

TABLE II. Radial matrix elements $\langle n,l|r|n,l\rangle$ for hydrogen, thl denotes the calculated numerical results of Li *et al.* [9], ths denotes our calculated numerical results.

n	l	Exact results (a.u.)	thl (a.u.)	ths (a.u.)
6	5	39.0	38.999999999981	39.000000000001
10	5	135.0	134.99999999997	135.00000000004
20	5	585.0	584.99999999994	585.00000000006
30	5	1335.0	1334.9999999998	1334.9999999998
40	5	2385.0	2384.9999999998	2385.0000000003
50	5	3735.0	3734.9999999998	3735.0000000001
60	5	5385.0	5385.000016	5385.0000000002
70	5	7335.0	7335.54	7335.000000002
80	5	9585.0		9585.000000001
90	5	12135.0		12134.999999992
100	5	14985.0		14985.00000003
105	5	16522.5		16522.49999997
110	5	18135.0		18134.99999997
115	5	19822.5		19822.50000009
120	5	21585.0		21584.9999997
125	5	23422.5		23422.5000004
130	5	25335.0		25334.9999994
135	5	27322.5		27322.500001
140	5	29385.0		29384.999992
145	5	31522.5		31522.500002
150	5	33735.0		33734.997

The sodium Stark maps in the neighborhood of $n=20$ ($|m|=0,1$) are shown in Figs. 1 and 2, respectively. For simplicity, the notation (n,l) represents the states that connect adiabatically to the field-free state of principal quantum number n and angular momentum quantum number l, and (n,l_1-l_2) denotes a Stark manifold which contains $(n,l_1),(n,l_1+1),\ldots,(n,l_2)$.

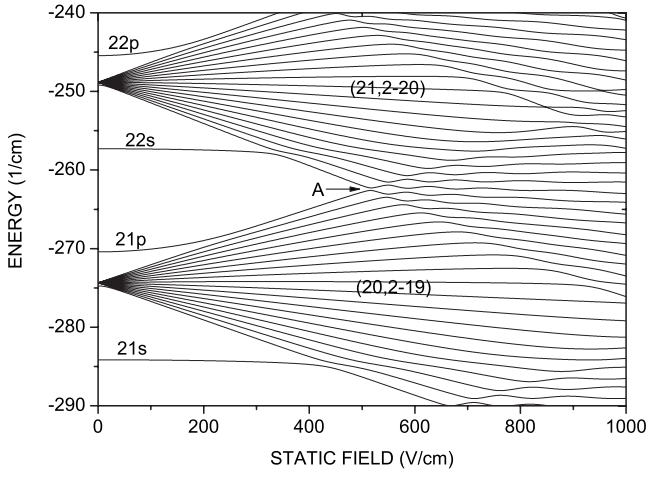

FIG. 1. Stark energy levels of sodium in the vicinity of $n=20$ ($|m|=0$). *A* is the initial anticrossing between Stark manifold 20 and 21.

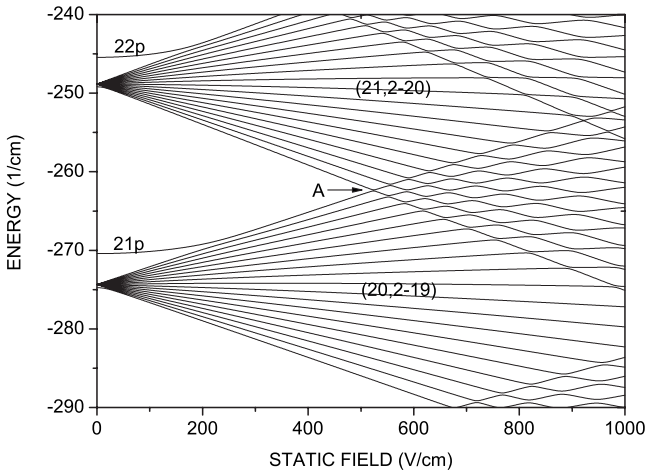

FIG. 2. Stark energy levels of sodium in the vicinity of $n=20$ ($|m|=1$). *A* is the initial anticrossing between Stark manifold 20 and 21.

In investigating the anticrossing, the energy difference of two relevant levels is a function of the electric field. The minimal value of this function is at the point where the position of anticrossing is defined, and the width of anticrossing is defined as this minimal value.

TABLE III. Calculated positions of the first anticrossing between Stark manifold n and $n+1$ in Na for the case of $|m|=0-2$, n ranging from 15 to 35. thl denotes the calculated positions of Li [7]. ths denotes our calculated positions. All values are given in V/cm.

	$\|m\|=0$		$\|m\|=1$		$\|m\|=2$	
n	thl	ths	thl	ths	thl	ths
15	2163	2163	2194	2195	2365	2366
16	1569	1569	1592	1592	1707	1707
17	1160	1160	1177	1177	1257	1257
18	873.0	873.1	885.6	885.8	941.4	941.6
19	667.0	667.2	676.6	676.7	716.7	716.8
20	516.8	516.9	524.1	524.2	553.4	553.5
21	405.4	405.4	411.0	411.1	432.7	432.8
22	321.6	321.6	326.0	326.1	342.4	342.4
23	257.8	257.8	261.2	261.3	273.7	273.8
24	208.5	208.6	211.3	211.4	220.9	221.0
25	170.2	170.2	172.4	172.4	179.9	180.0
26	140.0	140.0	141.8	141.8	147.7	147.7
27	116.0	116.0	117.5	117.5	122.2	122.2
28	96.81	96.83	98.00	98.02	101.80	101.80
29	81.29	81.30	82.27	82.28	85.32	85.34
30	68.65	68.67	69.47	69.49	71.96	71.97
31	58.32	58.33	58.99	59.01	61.03	61.04
32	49.79	49.80	50.35	50.37	52.03	52.05
33	42.71	42.72	43.19	43.20	44.59	44.59
34	36.81	36.82	37.22	37.22	38.38	38.39
35	31.86	31.87	32.21	32.21	33.18	33.19

TABLE IV. Calculated widths of the first anticrossing between Stark manifold n and $n+1$ in Na for the case of $|m|=0-2$, n ranging from 15 to 35. thl denotes the calculated widths of Li [7]. ths denotes our calculated widths. All values are given in 1/cm.

	$\|m\|=0$		$\|m\|=1$		$\|m\|=2$	
n	thl	ths	thl	ths	thl	ths
15	1.211	1.203	5.621−1	5.532−1	1.075−2	6.747−3
16	9.016−1	8.956−1	4.120−1	4.051−1	7.235−3	4.362−3
17	6.836−1	6.789−1	3.072−1	3.020−1	4.981−3	2.886−3
18	5.268−1	5.231−1	2.329−1	2.288−1	3.503−3	1.950−3
19	4.120−1	4.090−1	1.791−1	1.758−1	2.514−3	1.342−3
20	3.263−1	3.239−1	1.395−1	1.369−1	1.826−3	9.390−4
21	2.615−1	2.596−1	1.100−1	1.079−1	1.351−3	6.671−4
22	2.118−1	2.102−1	8.764−2	8.592−2	1.013−3	4.806−4
23	1.732−1	1.719−1	7.053−2	6.911−2	7.692−4	3.505−4
24	1.429−1	1.418−1	5.726−2	5.609−2	5.911−4	2.587−4
25	1.188−1	1.179−1	4.688−2	4.591−2	4.597−4	1.929−4
26	9.956−2	9.877−2	3.868−2	3.786−2	3.617−4	1.453−4
27	8.401−2	8.331−2	3.221−2	3.145−2	2.851−4	1.104−4
28	7.130−2	7.072−2	2.689−2	2.630−2	2.323−4	8.458−5
29	6.088−2	6.038−2	2.623−2	2.213−2	1.833−4	6.529−5
30	5.227−2	5.184−2	1.915−2	1.873−2	1.486−4	5.076−5
31	4.511−2	4.474−2	1.630−2	1.593−2	1.213−4	3.974−5
32	3.912−2	3.879−2	1.395−2	1.362−2	9.968−5	3.129−5
33	3.407−2	3.379−2	1.198−2	1.171−2	8.243−5	2.479−5
34	2.980−2	2.955−2	1.036−2	1.010−2	6.864−5	1.974−5
35	2.617−2	2.595−2	8.897−3	8.755−3	5.741−5	1.580−5

We calculate the positions and widths of the initial anticrossings between Stark manifold n and $n+1$ in sodium for the case of $|m|=0-2$ and $n=15-70$. In our calculation, we use the B-spline basis with order $k=9$ and number $N=1000$. The knot sequence is determined by exponential sequence. In this way, the B-spline basis can best represent the zero-field behavior. The basis is chosen from the zero-field wave functions from $n-4$ to $n+7$ manifolds. This choice has warranted the convergence of the related positions and widths.

The results of the positions and widths with n from 15 to 35 are presented in Tables III and IV, respectively. For comparison with the corresponding data of Li [7], his results are also listed in Tables III and IV. We can see from Tables III and IV that our theoretical values are in good agreement with Li. However, our calculated widths are narrower than those of Li in the case of $|m|=2$. The reason may be that different model potentials are chosen for two calculations. We need experiments to confirm which model potential is better.

The calculated positions and widths of the first anticrossings for highly excited Stark states of Na with principal quantum number n ranging from 35 to 70 are listed in Tables V and VI, respectively. In order to compare the calculated locations of anticrossings with the $1/3n^5$ scaling law [7], the field positions of $1/3n^5$ are also listed in Table V. From Table V, we can see that all fields of the initial anticrossings follow the $1/3n^5$ scaling law. From Table VI, we can see that

TABLE V. Calculated positions of the first anticrossing between Stark manifold n and $n+1$ in Na for the case of $|m|=0-2$, n ranging from 36 to 70. The positions from the scaling law $1/3n^5$ in atomic units or $1.71\times10^9 n^{-5}$ in units of V/cm are also listed. All values are given in V/cm.

n	$\|m\|=0$	$\|m\|=1$	$\|m\|=2$	$1/3n^5$
36	27.694	27.990	28.813	28.280
37	24.161	24.414	25.112	24.660
38	21.155	21.373	21.967	21.581
39	18.587	18.775	19.283	18.953
40	16.384	16.547	16.983	16.700
41	14.487	14.629	15.004	14.760
42	12.848	12.972	13.296	13.084
43	11.426	11.535	11.816	11.632
44	10.189	10.285	10.529	10.369
45	9.109	9.193	9.407	9.267
46	8.164	8.238	8.426	8.302
47	7.334	7.400	7.564	7.456
48	6.604	6.662	6.807	6.711
49	5.959	6.010	6.138	6.054
50	5.388	5.434	5.547	5.472
55	3.350	3.377	3.440	3.397
60	2.171	2.187	2.225	2.199
65	1.456	1.467	1.490	1.474
70	1.006	1.013	1.028	1.017

the widths for $|m|=2$ are much narrower than the ones for $|m|=0,1$. This is because the $|m|=2$ states are composed of zero-field $l\geqslant 2$ states, all of which have small quantum defects, and as a result, the avoided crossings between different n are very small.

Another important potential for Na^+-e system is given by Peach [18] and has the following form:

$$V_e(x) = -\frac{z}{x} - \frac{Z}{x}(1+\delta x+\delta' x^2)\exp(-\gamma x) - \frac{\alpha_d}{2x^4}\omega_2(\beta x) - \frac{\alpha_q'}{2x^6}\omega_3(\beta' x), \tag{9}$$

in which the function $\omega_n(y)$ is defined by

$$\omega_n(y) = [\chi_n(y)]^2 \tag{10}$$

and

$$\chi_n(y) = 1 - \exp(-y)\sum_{m=0}^{n}\frac{y^m}{m!}. \tag{11}$$

The optimized parameters in (9)–(11) are listed in Table VII (reproduced from Table 1 of Ref. [18]).

Both the potential of Peach and the potential of Marinescu *et al.* with angular momentum $l=0$ and 5 are presented in Figs. 3(a) and 3(b), respectively. We can see that there is almost no difference between two potentials at large values of R, especially for higher angular momentum. But at small

TABLE VI. Calculated widths of the first anticrossing between Stark manifold n and $n+1$ in Na for the case of $|m|=0-2$, n ranging from 36 to 70. All values are given in 1/cm.

n	$\|m\|=0$	$\|m\|=1$	$\|m\|=2$
36	2.287−2	7.618−3	1.270−5
37	2.023−2	6.654−3	1.025−5
38	1.795−2	5.832−3	8.312−6
39	1.598−2	5.129−3	6.763−6
40	1.427−2	4.526−3	5.521−6
41	1.278−2	4.006−3	4.521−6
42	1.148−2	3.555−3	3.713−6
43	1.033−2	3.165−3	3.058−6
44	9.325−3	2.824−3	2.524−6
45	8.435−3	2.527−3	2.088−6
46	7.648−3	2.266−3	1.731−6
47	6.949−3	2.037−3	1.437−6
48	6.327−3	1.836−3	1.194−6
49	5.771−3	1.657−3	9.938−7
50	5.275−3	1.500−3	8.277−7
51	4.830−3	1.359−3	6.900−7
52	4.430−3	1.235−3	5.755−7
53	4.070−3	1.123−3	4.798−7
54	3.746−3	1.024−3	3.992−7
55	3.452−3	9.349−4	3.322−7
60	2.346−3	6.072−4	1.290−7
65	1.645−3	4.081−4	4.469−8
70	1.184−3	2.825−4	8.267−9

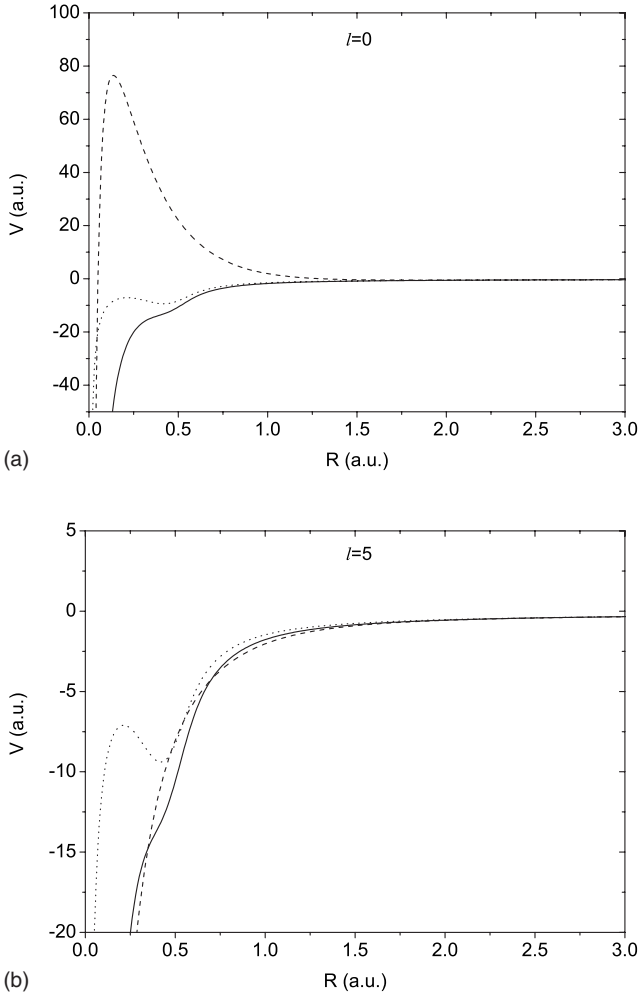

FIG. 3. (a) The parametric model potential [16] and the pseudopotential [18] for Na^+-e system with $l=0$. The solid line denotes the parametric model potential curve; the dotted line denotes the parametric model potential curve with the radial charge $Z_l(r)=1$; the dashed line denotes the pseudopotential curve. (b) The parametric model potential [16] and the pseudopotential [18] for Na^+-e system with $l=5$. The solid line denotes the parametric model potential curve; the dotted line denotes the parametric model potential curve with the radial charge $Z_l(r)=1$; the dashed line denotes the pseudopotential curve.

values of R, the two potentials differ very much, as indicated in Fig. 3(a). In order to see the effect of the different potential on the radial matrix elements, we calculate the radial matrix elements of sodium using the two potentials. The results are listed in Tables VIII and IX for angular momentum $l=0$ and 5, respectively. Table VIII shows that the difference of the radial matrix elements from different potentials is obvious for the case of $l=0$. However, Table IX shows the radial matrix elements with potential of Marinescu *et al.* are almost the same as ones with the potential of Peach for the case of $l=5$. This is easy to understand if we notice that there is a relative large difference between two potential curves for the case of $l=0$ in Fig. 3(a) but the potential curve of Marinescu *et al.* is almost the same as the one of Peach for the case of $l=5$ in Fig. 3(b).

For very large quantum numbers, the outer electron is far from the core and $Z_l(r)=1$ in Eq. (3) should be a good approximation, i.e., Coulomb potential plus long-range potential only in Eq. (2). To check this fact, we calculate the radial matrix elements of sodium using the potential of Marinescu *et al.* with $Z_l(r)=1$. The results for this case are also listed in Tables VIII and IX. We can see from Table VIII that there is a relative large difference between the radial matrix elements

TABLE VII. Parameters for the l-dependent pseudopotential of Na (reproduced from Table 1 of Ref. [18]).

	δ	δ'	γ	Z	z	α_d	α'_q	β	β'
$l=0$	−22.196651	−1.816006	4.228122						
$l=1$	−5.110092	−0.076640	2.945816	10	1	0.92389	0.857369	4.668978	3.157998
$l\geqslant 2$	−0.378834	0.341705	2.708505						

TABLE VIII. Diagonal radial matrix elements $\langle n,l|r|n,l\rangle$ for sodium, th1 denotes the calculated numerical results using the potential of Marinescu *et al.* [16], th2 denotes the numerical results using the potential of Marinescu *et al.* with the radial charge $Z_l(r)=1$, th3 denotes the numerical results using the potential of Peach [18].

n	l	th1	th2	th3
1	0	0.1621558908200	0.5899312538364	4.0919183456970
2	0	0.7791227731086	3.5949970382992	10.549081323874
3	0	4.0785280106979	9.7499294638674	20.005972022747
4	0	10.545661887702	18.900853810035	32.462476143000
5	0	20.003780864688	31.050824148270	47.918837132488
10	0	112.28457174267	136.79858998351	170.20017529766
15	0	279.56409857211	317.54595834311	367.48138934389
20	0	521.84355726495	573.29329582058	639.76258973392
30	0	1231.4024469083	1309.7879565742	1409.3249832890
50	0	3550.5202117411	3682.7772701072	3848.4497659530
70	0	7069.6379745311	7255.7665827504	7487.5745479457
100	0	14598.314614374	14865.250564669	15196.261735616
130	0	24826.991334075	25174.734619056	25604.948977079
150	0	33146.108349286	33547.724476749	34044.058904625

with the full potential and ones with $Z_l(r)=1$ for the case of $l=0$, even if the principal quantum number is as large as $n=150$. We can understand this result if we note that there are the penetration and polarization for the case of $l=0$, even if the principal quantum numbers are large. We can also see from Table IX that the radial matrix elements with the full potential are almost the same as ones with $Z_l(r)=1$ for the case of $l=5$ since there is almost no penetration and polarization for this case. We conclude that $Z_l(r)=1$ in Eq. (3) could be used when both the angular momentum quantum number and the principal quantum number are large.

Summarizing, in this paper, we report the approach that can be used to calculate the radial matrix elements of alkali metal Rydberg states with principal quantum number n up to 145. They are needed to calculate the transition matrix elements, radiative lifetimes, oscillator strengths and polarizabilities for alkali metal Rydberg states. The multiphoton ionization of alkali metal atoms in strong microwave fields is taken as multistep or rate-limiting step processes; and the ionization threshold is determined by the first transition step [2]. Each step is taken as a multiphoton transition process [3]. To calculate the multiphoton transition, the radial matrix

TABLE IX. Diagonal radial matrix elements $\langle n,l|r|n,l\rangle$ for sodium, th1 denotes the calculated numerical results using the potential of Marinescu *et al.* [16], th2 denotes the numerical results using the potential of Marinescu *et al.* with the radial charge $Z_l(r)=1$, th3 denotes the numerical results using the potential of Peach [18].

n	l	th1	th2	th3
6	5	38.999347056669	38.999335314732	38.997608594992
7	5	58.499500604121	58.499477081881	58.497100982619
8	5	80.999490599985	80.999456877204	80.996626311552
9	5	106.49944770492	106.49940512279	106.49616834578
10	5	134.99939590475	134.99934540297	134.99571957878
15	5	322.49911160361	322.49902783661	322.49352645786
20	5	584.99881930748	584.99870565217	584.99135672756
30	5	1334.9982311779	1334.9980595613	1334.9870284596
40	5	2384.9976420847	2384.9974130030	2384.9827031175
50	5	3734.9970527706	3734.9967663297	3734.9783783790
70	5	7334.9958737247	7334.9954730971	7334.9697290657
100	5	14984.994099092	14984.993519846	14984.956761287
130	5	25334.992416926	25334.991732099	25334.943807141
150	5	33734.988079040	33734.969279223	33734.930611908

elements of an alkali metal Rydberg state with principal quantum number n up to 70 are also needed. We also calculate the theoretical positions and widths of the initial anticrossings between Stark manifold n and $n+1$ in sodium with principal quantum number n up to 70 using our approach that use B-spline basis set and a parametric model potential.

ACKNOWLEDGMENTS

We would like to thank Professor Baiwen Li, Professor Tingyun Shi, and Ellen Leigh. The project is sponsored by the Scientific Research Foundation for the Returned Overseas Chinese Scholars, State Education Ministry.

[1] T. N. Chakrabarty, J. Astrophys. Astron. **25**, 93 (2004).
[2] T. F. Gallagher, in *Atoms in Intense Laser Fields*, edited by M. Gavrila (Academic, New York, 1992), p. 67.
[3] C. R. Mahon, J. L. Dexter, P. Pillet, and T. F. Gallagher, Phys. Rev. A **44**, 1859 (1991).
[4] A. Krug and A. Buchleitner, Phys. Rev. A **72**, 061402(R) (2005).
[5] J. M. Menendez, I. Martin, and A. M. Velasco, J. Chem. Phys. **119**, 12926 (2003).
[6] Y. Li *et al.*, Opt. Commun. **253**, 338 (2005).
[7] Y. Li, Theor. Chem. Acc. **117**, 163 (2007).
[8] F. Gounand, J. Phys. (Paris) **40**, 457 (1979).
[9] Y. Li and B. Li, Z. Phys. D: At., Mol. Clusters **42**, 89 (1997).
[10] H. Bachau, E. Cormier, P. Decleva, J. E. Hansen, and F. Martin, Rep. Prog. Phys. **64**, 1815 (2001).
[11] J. Xi, L. Wu, X. He, and B. Li, Phys. Rev. A **46**, 5806 (1992).
[12] W. Liu, J. Xi, X. He, L. Wu, and B. Li, Phys. Rev. A **47**, 3151 (1993).
[13] J. Rao and B. Li, Phys. Rev. A **51**, 4526 (1995).
[14] C. Jin, X. Zhou, and S. Zhao, Commun. Theor. Phys. **44**, 1065 (2005).
[15] C. Jin, X. Zhou, and S. Zhao, Commun. Theor. Phys. **47**, 119 (2007).
[16] M. Marinescu, H. R. Sadeghpour, and A. Dalgarno, Phys. Rev. A **49**, 982 (1994).
[17] C. de Boor, *A Practical Guide to Spline* (Springer, New York, 1978).
[18] G. Peach, Comments At. Mol. Phys. **11**, 101 (1982).
[19] M. L. Zimmerman, M. G. Littman, M. M. Kash, and D. Kleppner, Phys. Rev. A **20**, 2251 (1979).